Review

Linking Experimental Models to Pathophysiology: Oxidative Stress and DNA Damage in Cardiovascular Diseases

Shahin Gavanji , Hazem Zaki , Priyadarshini Panjwani , Eman M. Othman *

Posted Date: 1 April 2026

doi: 10.20944/preprints202604.0024.v1

Keywords: cardiovascular; oxidative stress; in vitro; in vivo; assay; ROS

 doi:10.20944/preprints202604.0024.v1

Review

Linking Experimental Models to Pathophysiology: Oxidative Stress and DNA Damage in Cardiovascular Diseases

Shahin Gavanji [1], Hazem Zaki [2], Priyadarshini Panjwani [3] and Eman M. Othman [4,5,*]

[1] Department of Plant Biotechnology, Medicinal Plants Research Centre, Isfahan (Khorasgan) Branch, IslamicAzad University, Isfahan, Iran

[2] Faculty of Pharmacy, Deraya University, Minia 61111, Egypt

[3] Nonclinical Development unit, CSL Innovation GmbH, Marburg, Germany

[4] Department of Biochemistry, Faculty of Pharmacy, Minia University, Minia 61519, Egypt

[5] Cancer Therapy Research Center (CTRC), Department of Biochemistry-I, Biocenter, University of Wuerzburg, Wuerzburg, Germany

* Correspondence: eman.sholkamy@uni-wuerzburg.de

Abstract

There has been an immense concern in the healthcare industry about the globally raising rate of cardiovascular disease (CVD). As per recent WHO reports, CVD is the leading cause of disability, hospitalization and premature death. Studies indicate oxidative stress negatively impacts heart and vascular system which could potentially lead to myocardial infarction, hypertension, cardiomyopathies, atherosclerosis and diabetic heart failure, highlights its significance as prognostic indicator in cardiovascular conditions Currently, Oxidative stress and its negative effect can be accessed by many multiple experimental tools in both, in-vitro and in-vivo settings. Nowadays, many common experimental assays are used for in-vitro and in-vivo evaluation of oxidative stress and its negative effects on the cardiovascular system. This review aims to serve as a comprehensive guide for researchers seeking to evaluate impact of oxidative stress on DNA damage in CVD utilizing standardized methods published by leading institutions. To achieve this, we analyzed 208 relevant articles from prominent databases such as Scopus, PubMed, ScienceDirect, etc. summarizing experimental validation of oxidative stress measurements from 1955 to the present. Oxidative stress–induced DNA damage is a key driver of cardiovascular disease progression, yet experimental approaches to study it remains highly variable. This review systematically summarizes established in-vitro and in-vivo models, oxidative stress inducers, and analytical assays used in cardiovascular research. By integrating mechanistic insights with standardized methodologies, it provides a practical framework to guide model selection, improve reproducibility, and enhance translational relevance. This work serves as a concise reference for researchers investigating redox biology, cardiovascular pathology, and antioxidant-based therapeutic strategies.

Keywords: cardiovascular; oxidative stress; in vitro; in vivo; assay; ROS

1. Introduction

Medical experts around the world are increasingly concerned about the raising rate of cardiovascular disease (CVD). It's the leading cause of early death, disability and put huge strain on healthcare systems and economies. In fact, CVD is considered the most expensive disease with an estimated indirect cost of $237 billion each year [1,2].

Research shows that many common risk factors like smoking, drinking alcohol, lack of physical activity, poor diet, hormonal changes due to stress, lack of proper sleep, obesity, and hypertension can lead to CVD [3], These factors are known to increase oxidative stress in body [4–6]. When body

 doi:10.20944/preprints202604.0024.v1

produces too many reactive oxygen species (ROS) and doesn't have enough antioxidants to balance them out it leads to oxidative stress. This can damage important molecules like DNA, lipids, and proteins [7,8] which contributes to many diseases including cancers metabolic disorders and hormonal conditions leading to CVD [9,10]. Oxidative stress negatively impacts heart and blood vessels and can lead to conditions such as myocardial infarction, atherosclerosis, and diabetic heart failure [11,12]. The main sources of ROS in the heart include enzymes such as xanthine oxidoreductase, Monoamine oxidases (MAO), NADPH oxidases (NOXes), mitochondria, Cytochromes P450 (CYP) and nitric oxide (NO) synthases [7,9]. Tracking oxidative stress in blood, serum, plasma has helped researchers identify biomarkers that play key role in development of heart diseases. These markers play significant role in coronary artery disease (CAD) development and can also be used to predict disease progression of CVD [13]. For example, Serum lipid hydroperoxides (LOOHs) are primary products of fatty acid peroxidation, while Malondialdehyde (MDA) - a stable end product of lipid peroxidation (LP) result from an interaction between radical species and PUFAs [14]. Elevated levels of LOOH and MDA have been associated with cardiovascular risk factors like smoking and diabetes mellitus therefore, highlighting their utility to predict primary and secondary CVD [15,16]. Currently various in-vitro and in-vivo assays are employed to access oxidative stress and its detrimental impact on the CVD. These standard testing methods are instrumental not only in evaluating CVD risk but also screen for novel drugs with antioxidant activity. Over past decade, several studies focused on development and validation of such assays offering practical tools to study and access oxidative stress in CVD and to design novel antioxidant based therapeutic strategies. Our review provides comprehensive guidance for researchers by summarizing widely adopted and standardized assays used globally across academic, institutional, preclinical and clinical research settings.

2. Methods

To put together this review article, we explored wide range of publications, scientific protocols, and books available on major research databases Web of Science PubMed, Scopus, Google Scholar and, Science Direct. We focused on keywords such as oxidative stress assays and ROS in cardiovascular diseases, in-vitro and in-vivo studies, and methods to assess oxidative stress and DNA damage in CVD. We used two sets of criteria to select the source; first was the broad filter that included in-vitro and in-vivo methods for measuring oxidative stress. The second was more detailed focusing on studies specifically testing oxidative stress in CVD and heart failure. Our comprehensive search includes publication dating back to 1955 to ensure that we captured both foundational work and recent advancements (Figure 1).

 doi:10.20944/preprints202604.0024.v1

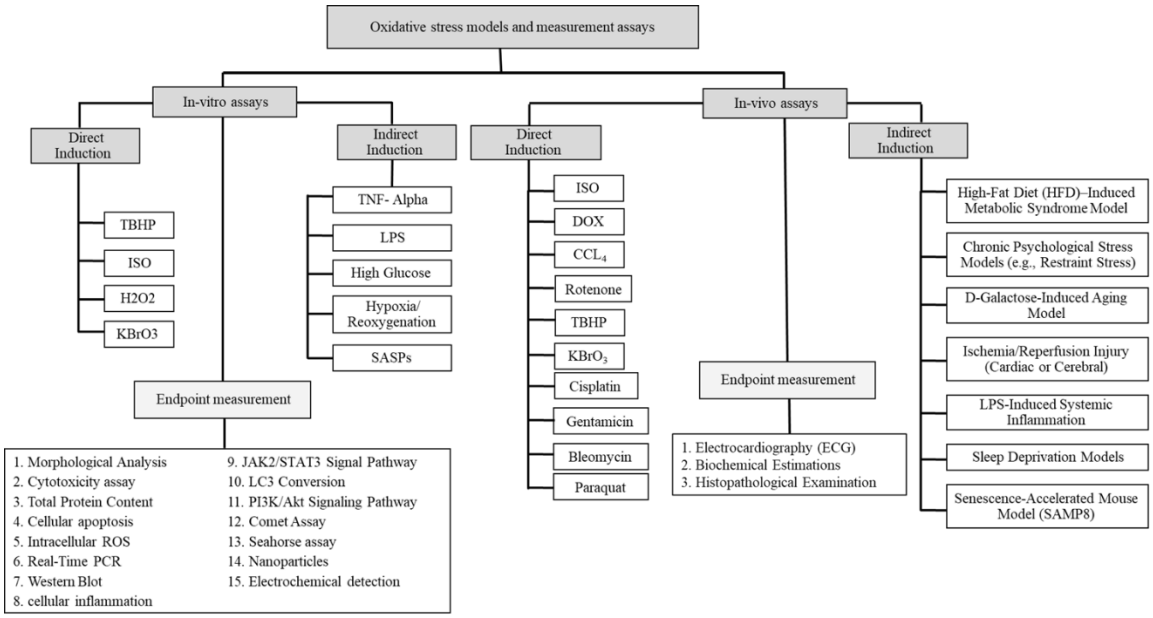

Figure 1. Methods for in-vitro and in-vivo oxidative stress induction and evaluation.

3. Experimental In-Vitro Models

One of the key steps in pre-clinical research on CVD is evaluating the detrimental effects of oxidative stress on the heart and vascular system. Oxidative Stress can lead to various cellular abnormalities that ultimately contribute to cardiac dysfunction. To study these effects, it is important to select an appropriate in-vitro model that allows precise control over experimental conditions [17]. In-vitro models including primary or induced pluripotent single cardiac cell, 2D and 3D cultures, tissue culture, and microfluidic platforms are essential tools. They support researchers to explore the molecular mechanisms of ROS, along with its interaction with cells and gather valuable insights before moving on to in-vivo assay and de-risk major in-vivo studies by contributing to 3R (Table 1). A critical factors for obtaining reliable results is selecting the right cell lines [18]. The choice depends on several factors, including the available laboratory equipment, type of in-vitro models, functional characteristics of the cells, and the specific goals of the assay (17, 18). A variety of cell-lines are commonly used in CVD, including cell-lines like AT-1 [19], HL-1 [20], AC [21], and H9c2 [22], primary neonatal and adult cardiomyocytes [23,24] and stem or progenitor cells [25]. Among these the H9c2 cell-line has been most frequently used in CVD [22,26,27]. Derived from BD1X rat heart tissue, H9c2 cell line exhibits several properties of skeletal muscle and offers a versatile platform to investigate oxidative damage and its role in cardiac systems [28].

Table 1. In-vitro models for assessment of oxidative stress in the cardiovascular system.

In vitro *models*	*Advantages*	*Disadvantages*
Cardiac single cell	• provide information about characteristic of each cardiac cell (20) • Help us to quantify the various mechanical properties in individual cells [29] • It can help to evaluate the electrophysiology of a of single cardiomyocytes (CMs) [30]	• The structure and lattice-like network misalignment of myofibrils can limit their efficiency of contractile activity modeling [31] • There is cell-to-cell differences and variations in the cell size, myofibril alignment myocyte type, shape which cause the incorrect measurements in the result [31] • The isolated cardiomyocytes have different responses to drugs in cells and

 doi:10.20944/preprints202604.0024.v1

		groups and can lead to different results [17].
Two-dimensional (2D) cell cultures	• This method has a closer condition to the in vivo state [32] • It helps us to assess the molecular signaling pathways [32] • Useable for cardiotoxicity evaluations and gene therapy approaches [33,34]	• Sometimes has variations in the cell morphology and polarity [35] • The cellular and extracellular environments have problems in interaction (30) • May offer the misleading results [35]
Three- dimensional (3D) cell cultures	• Express a wide range of proteins in the CMs culture in comparison with 2D cultures [36]	• The materials which have been used in the construction of 3D cardiac cultures can reduce cell survival rates and increase the thickness [37] • Geometric design limitation [17]
Coculture	• Simple [17,38] • It provides information to study the cell–cell interactions [39]	• The continuous cell lines affection which sometimes show phenotypes that have not observed in the primary cells [40]
Microfluidic cell culture	• It helps us to have cellular behavior information • Provide a platform to study the physiology of normal heart cell and help to create the disease for therapeutic evaluation [35] • It provides precise control over cell culture [39]	• Sometimes accompanying of cell cultures with microfluidic devices can face to problem [41]

4. Direct Inducers of Oxidative Stress In-Vitro

4.1. Tert-Butyl Hydroperoxide (TBHP)

TBHP is one of the most commonly used compounds for investigating induction of oxidative stress in in-vitro models. It is well-known for its ability to trigger damage and apoptosis in cardiomyocyte [42,43]. The H9c2 myocardial cell line is widely considered an ideal model for studying oxidative stress and DNA damage in cardiovascular research. To perform this assay, H9c2 cells are cultured in Dulbecco's modified Eagle medium (DMEM) supplemented with 10% fetal bovine serum (FBS), 100 µg/ml streptomycin, 100 U/ml penicillin, 1.5 g/L sodium bicarbonate and 4 mM L-glutamine. The cells are maintained in humidified incubator at 37°C with 5% CO_2 and 95% O_2. After 2-3 passages of the stock cultures cells are seeded into 96-well plates at a density of 5.0×10^3 cells per well. Once attached, cells are treated with 150-200 µM TBHP for 1 h, depending on read-out planned for the end point measurement. This provides a consistent and reliable setup for investigation of oxidative stress antioxidant strategies [44,45].

4.2. Isoproterenol (ISO)

ISO-induced myocardial ischemia is a classical model used to evaluate the cardio-protective effects of various pharmacological agents. ISO causes severe oxidative stress in the myocardium, leading to infarct-like necrosis of the myocardium.

To perform this assay, the H9c2 cells are cultured and divided into several groups: negative control, ISO-treated (50 µmol/L), positive control (0.1 mmol/L captopril), and treatment groups with different concentrations of test item with predicted antioxidant properties. All groups incubated for 24 h. Afterwards, all groups except the negative control group are treated with 50 µmol/L ISO, and incubated for 48 h. Depending on the endpoint, read-out is conducted and analyzed [46–49].

 doi:10.20944/preprints202604.0024.v1

4.3. Hydrogen Peroxide (H_2O_2)

H_2O_2 is a commonly used ROS inducer for generating oxidative stress and cellular damage in various in vitro models [50]. Endogenous H_2O_2 in immune and vascular smooth muscle cells contributes to generation of oxidative stress which leads to endothelial dysfunction and development of various vascular diseases [51]. To perform this assay, seed H9c2 cells in 96-well plates at a density of 5×10^3 cells per well, allowing them to reach logarithmic growth phase. Then, divide them in different groups and treat them with 200-400 μM of H_2O_2 for 24 h, upon treatment, cells can be used for subsequent experiments [52].

4.4. Potassium Bromate ($KBrO_3$)

$KBrO_3$ is a food additive that has been used commonly used in production of drinking water disinfected with ozone [53]. Due to its strong oxidizing properties, $KBrO_3$ can act as an inducer of oxidative stress leading to lipid peroxidation and DNA damage [54]. The free radicals generated by KBrO3 are known cardiac toxins, and heart is very sensitive to its effect [55,56].

To perform this assay, seed the H9c2 cells in 96-well plates at a density of 5×10^3 cells per well, and allow them to reach logarithmic growth phase. Then, divide them into the different groups and treat them with 250 μM $KBrO_3$. Incubate the cells in humidified incubator at 37°C with 5% CO_2 and 95% O_2 for 72 h [57].

4.5. Indirect Inducers of Oxidative Stress in In-Vitro

4.5.1. Tumor Necrosis Factor-Alpha (TNF-α)

TNF-α is a pro-inflammatory cytokine that promotes oxidative stress via activation of mitochondrial dysfunction and NADPH oxidase pathways. It plays a central role in enhancement of ROS induction in various cardiac and vascular models.

To perform this assay, H9c2 cells are cultured and seeded into 96-well plates at a density of 5×10^3 cells per well. Once attached, cells are treated with 10–50 ng/mL TNF-α for 24 h. The resultant oxidative stress can be measured through ROS-specific fluorescent probes and antioxidant enzyme activity assays [58].

4.5.2. Lipopolysaccharide (LPS)

LPS, a structural component of Gram-negative bacterial walls, is a widely used stimulator of inflammation-induced oxidative stress. Upon binding to TLR4, LPS activates transcription factors like NF-κB, which enhances intracellular ROS generation and impairs mitochondrial integrity.

To model this in-vitro, H9c2 cells are treated with 1 μg/mL LPS for 24–48 h under standard conditions. The LPS model is particularly useful in evaluating antioxidant properties of natural and synthetic compounds [59].

4.5.3. High Glucose (HG)

Chronic exposure to high glucose mimics diabetic hyperglycemia and induces oxidative stress through enhanced mitochondrial ROS production and suppression of antioxidant pathways. This model is frequently used in diabetic cardiomyopathy research.

To perform this assay, H9c2 cells are cultured in DMEM supplemented with 25- or 33-mM D-glucose for 48–72 h. The cells are then analyzed for markers of oxidative damage such as increased ROS, lipid peroxidation, and changes in GSH levels [60].

4.5.4. Hypoxia/Reoxygenation (H/R)

The hypoxia/reoxygenation model simulates ischemia-reperfusion injury in vitro, where the sudden influx of oxygen leads to a burst of ROS formation, especially from the mitochondria.

For this assay, H9c2 cells are exposed to hypoxic conditions (1% O_2) for 4–6 h using a hypoxia

 doi:10.20944/preprints202604.0024.v1

chamber or gas control incubator, followed by reoxygenation in normoxic conditions (21% O_2) for 2–24 h. This model closely mimics clinical scenarios such as myocardial infarction or stroke [61].

4.5.5. Senescent Cell Co-Culture

Senescent cells are metabolically active and exhibit a senescence-associated secretory phenotype (SASP), which includes pro-oxidant cytokines and matrix-degrading enzymes. This microenvironment leads to increased oxidative burden in neighboring cells.
To simulate this, H9c2 cells can either be co-cultured with senescent fibroblasts or treated with 0.2–0.5 μM doxorubicin for 24 h to induce senescence. After 48–72 h of exposure, oxidative stress parameters can be assessed [62].

Table 2. Common induction of oxidative stress in cardiac cell culture (H9c2).

Inducers	*Experimental observation*	*Molecular Mechanisms*	*Inducer dose*	*EC50/appotosis*
TBHP	• Downregulate the Bcl2 as an anti-apoptotic protein and upregulate the Bax protein as an apoptotic protein [45] • It can decline the cellular antioxidant enzymes in the cell [45] • Induce cell death [45] • Rhodamine123 fluorescence will decrease by 66% [45]	• Provided by cytochrome P450, which can lead to generate of peroxyl (LOO○) and alkoxyl (LO○) radicals, that can initiate the lipoperoxidation (LPO) of membrane phospholipids with devastating reactions [63] • Depletion of GSH by oxidation to its disulphide form (GSSG) [64] • It can express the 21 genes that are involved in ROS [65]	• 150 μM [45]	• >150 μM [66]
ISO	• The cells are obviously hypertrophic [46] • Increase the mRNA expression levels of ANP, β-MHC and BNP [46] • It decreases the level of GSH and SOD and increase the MDA [46] • Increase the level of IL-6 and TNF-α [46]	• It causes an imbalance of antioxidants and oxidants in the myocardium that can lead to myocardial injury [67,68] • It enhances the phosphorylation levels of STAT3 and JAK2 [46]	• 50 $\mu mol \cdot L^{-1}$ [46]	• 50-300 μM [51]
H2O2	• It induces hypertrophy in cells by affecting the ERK1/2 and Akt signaling pathways [52]	• It can induce the PI3K/Akt Signaling Pathway [52]	• 200-400 μM [52]	• 471.8±27.5 μM [52]
KBrO3	• The cell size will increase at concentrations of <250 μM [64]	• Increase the expression of two cardiac hypertrophy markers, including β-Myosin Heavy Chain (β-MHC) and the brain/B-type natriuretic peptides (BNP) [64]	• <250 μM [64]	• >300 μM [64]

 doi:10.20944/preprints202604.0024.v1

5. In-Vitro Assays for Oxidative Stress and DNA Damage in Cardiovascular Diseases

Morphological Analysis

The H9c2 myocardial cell line is a well-established model for in-vitro evaluation of oxidative stress. To examine morphological changes, the cells should be fixed and stained following the YF®488 labeled Phalloidin staining protocol.

Briefly, fix the several cells on ice using 4% paraformaldehyde solution for 15 min. Then wash gently with PBS. Permeabilize using 0.5% Triton X-100 in PBS at room temperature for 10 min, followed by another PBS wash. Dilute 5 µL YF®488 labeled Phalloidin stock solution in 200 µL PBS and incubate cells with this mixture for 30 min at RT. After staining, wash off extra dye with PBS. Finally, observe the morphological changes using 400× inverted fluorescence microscope. For analysis, randomly select four to six views from each sample and measure the cell - surface with Oplenic software [49,69–71].

6. Cytotoxicity Assay

To assess cell viability, MTT assay is commonly used. Breifly, pre-incubate H9C2 suspensions cells in DMEM within 96-well plates at a concentration of 5×10^4 cells/100 µl/well. Incubate overnight in humidified incubator at 37 °C with 5% CO_2. Next day, replace the culture medium with fresh medium contains different groups-such as negative controls, positive control and treatment groups. Cells are treated with different concentrations of oxidative stress inducers and vehicle controls. Incubate the cells under same conditions for 6 h. Post treatment, add 10 µl of 10% MTT solution to each well and incubate for 4 h at 37 °C. Once incubation is complete, remove the supernatants and dissolve the formazan crystals in 100 µl of solubilization solution. Measure the absorbance by microplate reader at 630 nm [72]. To calculate percentage of viable cells, use the following equation:

$$\text{Cell viability (\%)} = \left[\frac{\text{Mean OD}_{\text{sample}}}{\text{Mean OD}_{\text{blank}}}\right] \times 100$$

6.1. Determination of Total Protein Content

To assess total protein content, along with SOD, GSH, and MDA levels use the appropriate commercial test kit. For this assay, centrifuge different treatment groups such as- negative control, positive control and treatment groups. Treat cells with different concentrations of oxidative stress inducers and vehicle controls. Post incubation, centrifuge at 137g, collect cell pellet. Add 0.3 mL of normal saline to each pellet for total protein, GSH, SOD assay. For MDA assay, add 0.5 mL TBA working solution and follow manufacturer's instructions for accurate detection [73–75]

6.2. Determination of Cellular Apoptosis

To assess cellular apoptosis, begin by seeding cells at a concentration of 1×10^6. Wash the cells with Phosphate-buffered saline (PBS) and centrifuge cells at 200g for 5 min. Resuspend the resulting pellet in 100µl of Annexin-V-FLUOS labeling solution and incubate the cells at 15-25 °C for 15 min. After incubation, use a fluorescence microscope to analyze apoptosis. Detection performed using Annexin-V-FLUOS staining kit [76].

In addition to staining, quantitative real-time PCR (qRT-PCR) can be used to evaluate apoptosis at the gene expression level. This involves measuring the mRNA expression of key apoptotic markers including Bcl-2, Bcl-2/Bax, Bax, Caspase-3, Caspase-8 and, Caspase-9. Studies have shown that oxidative stress inducers promote apoptosis in cells raising the expression of pro-apoptotic genes such as Bax, Caspase-3, Caspase-8 and, Caspase-9 while reducing expression of anti-apoptotic genes like Bcl-2 and reducing Bcl-2/Bax ratio [77–80]

6.3. Determination of Intracellular ROS

 doi:10.20944/preprints202604.0024.v1

One of the key aspects of cellular behavior is its ability to respond to ROS within intracellular environment. The level of intracellular ROS can be measured by commercial ROS detection kits.

To perform this assay, harvest H9c2 cells and wash them thrice to remove traces of residual medium. Then add serum-free DMEM on cells. Stain them with 0.5 µL 100 mmol/L of 2′,7′–Dichlorofluorescin Diacetate (DCFDA), cell permeable fluorescent probe and place the cells in a dark for 30 min. The intracellular ROS level is then measured by flow cytometric evaluation of fluorescence intensity of DCFDA in cells [49,69,81].

7. Quantitative Real-Time PCR

To perform this assay, extract total RNA from H9c2 cells using RNA extraction kit. Then synthesize cDNA using cDNA synthesis kit. The mRNA expression levels of ANP, BNP, β-MHC, IL-6, TNF-α, Bax, Bcl-2, Caspase-3, Caspase-8 and Caspase-9 are then quantified using real time PCR [46].

8. Western Blot

For western blot assay, culture H9C2 cells (5×10^6 cells) for 24 h, and prepare several treatment groups including positive and negative controls. After treatment, extract total protein and determine concentration using BCA protein assay kit. Separate proteins by sodium dodecyl sulphate polyacrylamide gel electrophoresis (SDS-PAGE) and transfer them to polyvinylidene fluoride (PVDF) membranes. Block the membranes with skim milk and incubate overnight with primary antibodies against p-JAK2, JAK2, p-STAT3, STAT3, TNF-α, Caspase-3, PI3K, Akt, mTOR, LC3-II, LC3-I, and GAPDH. Finally, analysis band intensities with digital tools to evaluate variation in protein levels [46,82].

9. Measurement of Cellular Inflammation

To assess inflammation, quantitative Real-Time PCR to measure cellular mRNA expression levels of IL-6 and TNF-α was widely reported. Several studies demonstrated that expression of both, IL-6 and TNF-α increases in cells under oxidative stress. In addition, protein expression of TNF-α also rises in ROS treated groups. Therefore, this assay set-up is used to evaluate impact of ROS on IL-6 and TNF-α expression to measure anti-inflammatory effects of tested compounds [82–84].

10. Evaluation of JAK2/STAT3 Signal Pathway

Several studies demonstrated that oxidative stress inducers can induce cardiomyocyte hypertrophy (CH). To perform this assay, evaluate the protein expression levels of JAK2, p-JAK2, STAT3, and p-STAT3 in the different treatment groups.

Oxidative stress caused by increased levels of ROS have been shown to promote cardiac hypertrophy (add reference). To evaluate this, protein expressions of JAK2, p-JAK2, STAT3 and p-STAT3 have been measured in appropriate cellular systems[85–87].

11. Evaluation of LC3 Conversion

LC3 (Microtubule-associated protein 1A/1B-light chain 3) protein plays a central role in autophagy, the process by which cells break down and recycle damaged components to maintain equilibrium. LC3 is a key autophagosome marker and plays an important role in final stages of autophagosome formation. LC3-I is an inactive form of protein, floating in the cytoplasm. LC3-I gets converted to LC3-II, which attaches to the membrane of the autophagosome. The LC3-II/LC3-I ratio is commonly used to measure autophagy levels. LC3-II to LC3-I conversion can be detected with western blot [88–90].

11.1. PI3K/Akt Signaling Pathway

 doi:10.20944/preprints202604.0024.v1

PI3K/Akt/mTOR signaling pathway is key regulator for cell growth, survival, metabolism and autophagy, all of which are sensitive to increase in ROS levels. This pathway was very often reported in experimental models to investigate cellular response to oxidative stress. should be investigated. Western blot analysis to assess levels of PI3K, Akt, and mTOR in post treatment was performed. Reduction in levels of p-AKT and p-mTOR was indicative of oxidative stress in treated cells [91,92].

11.2. Comet Assay to Evaluate the Oxidative DNA Damage

Several methods exist to access oxidative DNA damage in mammalian cells under in-vitro conditions. Among them, the comet assay which is a simple and precise technique for quantifying DNA damage.

To perform this assay, seed the cells and mix them with 180µL of 0.5% low-melting agarose. Spread the mix onto fully frosted slides that have been already coated with a layer of 1% normal-melting agarose. Next, incubate slides in lysis solution composed of 0.1M EDTA, 10-g/L N-lauroylsarcosine sodium salt (pH 10), 2.5M NaCl, and 0.01M Tris, supplemented with 10% dimethyl sulfoxide (DMSO) and 1% Triton X-100 for 1 h at 4℃. After lysis, wash the slides and place them in the electrophoresis solution for 20 min. Then perform electrophoresis at 25 V and 300 Ma for 20 min. In the next step, neutralize the slides using 0.4M Tris buffer and dehydrate them in the cold methanol at -20℃ for 10 min. After dehydration, place the slides in the incubator at 37℃ to dry, and then store them at RT. Finally, stain the DNA with Gel Red/ DABCO (diazabicyclo-octane) solution and analyze the images from each slide. The main evaluation parameter in this assay is the percentage of DNA tail, which reflects the extent of oxidative damage [93].

12. Seahorse Assay

The Seahorse XFp Analyzer is widely used and is one of the most powerful tools for analyzing and evaluating cellular respiration. This assay allows measurement of the oxygen consumption rate (OCR), and extracellular acidification rate (ECAR) which provides valuable information about metabolic dysfunction, mitochondrial function and oxidative stress in viable cells [94]. One of the key advantages of this assay compared to traditional oxygraph methods is its requirement for a low number of cells, which is particularly useful for metabolic analysis in diseases associated with mitochondrial dysfunction, hence it is one of the most commercially used techniques in metabolism research [95].

To perform this assay, the Seahorse XF24 Extracellular Flux analyzer and its dedicated software are used. First, seed 2×10^4 H9c2 cells per well in XF24 cell culture plates. Incubate cells in XF assay medium, which is a modified DMEM medium, at 37 °C for 1 h. Next, cells are exposed to FCCP (a respiratory uncoupler) to measure maximal respiratory capacity of the cell, oligomycin, an ATP synthase inhibitor, to assess ATP-linked respiration, and rotenone plus antimycin A. Inhibitors of complex I and III to quantify non mitochondrial respiration. The results obtained after such analysis allow detailed profiling of mitochondrial function, which includes, basal respiration, ATP production, proton leak, maximal respiration, and spare respiratory capacity. These parameters are essential for evaluating the impact of oxidative stress and potential protective or therapeutic interventions on cellular metabolism. The main advantage of using Seahorse XFp Analyzer is the fact that it analyzes live cells, allowing compounds to be tested in a dose-dependent manner. This enables precise determination of their effects on cellular respiration and facilitates the calculation of lethal doses. [96,97].

13. Nanoparticles for Detection and Monitoring the Reactive Oxygen Species (ROS)

In recent years, growing number of research studies have focused on developing innovative tools for ROS detection, tracking and monitoring. To meet this need, various type of nanosensors and nanomaterials are designed to detect early signs of oxidative stress within biological systems [98]

 doi:10.20944/preprints202604.0024.v1

(Table 3). Numerous studies have shown that fluorescent nanomaterials, when combined with nanocarriers can significantly improve the optical performance of fluorescent probes and by minimizing photobleaching and enhancing signal stability [99–101]. The integration of nanomaterials in ROS detection offers several advantages including low toxicity, improved solubility, and precise customization of fluorescent imaging probes for specific biological environment [102]. Furthermore, the incorporation of nanomaterials into biosensors can enhance the physio-chemical properties of these analytical devices, improving their sensitivity, specificity and biocompatibility with in-vivo applications [103]. One of the emerging tools for evaluating ROS at tissue depth is photoacoustic (PA) imaging, a hybrid method that combines optical contrast with ultrasound resolution. PA imaging provides high spatial resolution and deep tissue penetration, making it a promising tool for ROS detection in live organisms [104,105]. Notably, photoacoustic sensors have been successfully used in cardiovascular research to monitor oxidative stress [106,107]. A Study by Jung et al. (2018) introduced thrombus-specific theranostic (T-FBM) nanoparticles which significantly enhance H_2O_2-triggered photoacoustic (PA) signals and also demonstrated antithrombotic effects of these molecules. [108]

Table 3. Application of nanomaterials in ROS measurement.

Nano Sensors *Nanomicelles/Nanopolymer/Carbon Nanotubes/ Metallic*	**Applications**	***Advantages***	***Disadvantages***	***References***
Luminescence	• Detection of nM ROS and H_2O_2 for intracellular and in-vivo models	• Highly favorable for tissue imaging by near-infrared • ROS measurement in Photodynamic therapy	• Unspecific	[109–113]
Fluorescent-quenching	• Detection of intracellular nM ROS	• No sign of Photobleaching • Precise and stable	• Metallic nanoparticles induced cytotoxicity	[114–118]
Surface-enhanced raman spectroscopy (SERS)	• Evaluation of Intracellular redox potential	• Stable • Reversible	• Exhibits the pH-sensitivity • Raman microscopy equipment required • Raman microscopy equipment, complicated assay design	[119,120]
ROS-dye encapsulation	• Detection nM and μM of ROS • Assessment of tumor associated ROS	• Higher signal and sensitivity • Efficient sub-cellular targeting	• Measurement problem for short-lived ROS due to encapsulation • Unstable and irreversible	[121–127]

 doi:10.20944/preprints202604.0024.v1

			• It is not specific	
Nano surface energy transfer (NSET)	• Detection of intracellular nM ROS	• Stability (PH Dependent) outside a reducing environment	• It is irreversible	[128]
Electrochemical	• Detection nM and μM of H_2O_2	• Fast detection • It has higher sensivity	• Unusable for in-vivo models	[129–136]

14. Electrochemical Detection

Electrochemical methods have emerged as precise, sensitive and straight forward way to measure the ROS under both, in-vitro and in-vivo conditions. In these methods, the platinized nanoelectrode are commonly used as ROS detectors due to high sensitivity and rapid response time. Electrochemical techniques are especially valuable in biological assessments, where they are applied to evaluate drug-induced ROS production. These methods are not only easy to use but also offer detection sensitivity, short incubation time and ability to detect low levels of intracellular ROS with high spatial resolution [137]. Advancements in nanotechnology have further enhanced the capabilities of these tools. The development of these nanoelectrodes has enabled single-cell electrochemical monitoring and analysis, opening new possibilities for assessing oxidative stress at cellular and sub cellular levels [138–142]. These ultra-fine nanoelectrodes can penetrate the cell membrane and directly measuring ROS levels within cellular organelles such as nucleus and mitochondria [140,143]. A notable example of this application was reported by Actis and colleagues in 2014, where they used carbon fiber disk-shaped nanoelectrode to measure ROS levels in melanoma cells demonstrating the potential of this technique for real-time intracellular ROS detection and tracking [144]. Further research has lead to the development of quartz nanopipette-based nanoelectrode, which offer enhanced precision compared to first generation nanoelectrodes in intracellular ROS measurement. These electrodes provide unique advantages in single-cell analysis, enabling researchers to measure oxidative stress triggers at individual cell level and its subcellular compartments, which will contribute immensely to study cancer and disease models. [145,146].

15. Electron Paramagnetic (Spin) Resonance (EPR/ESR)

The development of sensitive, specific and precise assay for ROS detection is essential for advancing our understanding of oxidative stress and its trigger in disease pathology [147,148]. One of the most widely recognized and reliable techniques for detecting free radicals is Spin trapping [149,150]. It is well-established technique for detection of short-lived free radicals which otherwise are too reactive, unstable and transient to observe or measure directly. In this technique, these fleeting radicals react with Spin traps – special chemical moiety that form stable covalent bond with free radicals resulting in the production of persistent nitroxide molecules that can be detected and measured using electron paramagnetic resonance (EPR), also known as electron spin resonance (ESR) [151]. This method is based on the principle of microwave radiation absorption by unpaired electrons in a magnetic field. Key components of the EPR system includes a microwave generator, and a resonator cavity, which work together to detect the magnetic signals generated by spin-labelled radicals leading to detection of ROS [152]. Among the most effective probes used in this method are cyclic hydroxylamines which are highly reactive with ROS. These probes are converted into stable nitroxide radicals, making them ideal for quantitative EPR analysis. Several factors enhance the efficiency of hydroxylamine-based spin probes in ROS detection including their reactivity, accumulation rate, membrane permeability, organelle-targeting ability and chemical stability [153–

 doi:10.20944/preprints202604.0024.v1

155]. Due to enhanced specificity and ability to detect real-time radical formation, EPR remains one of the gold-standard techniques for studying oxidative stress in both in-vitro and in-vivo systems.

16. Extracellular H_2O_2 Detection by Amplex Red

The Amplex Red assay is a widely used and reliable tool for detection of extracellular H_2O_2 in biological samples [156]. This assay is based on the oxidation of Amplex Red reagent (10-acetyl-3,7-dihydroxyphenoxazine) in the presence of horseradish peroxidase (HRP) producing highly fluorescent and stable compound resorufin. To perform the assay, transfer three aortic segments (approximately 2mm in length) into 96-well plate. Add 10 μmol/L Amplex Red with 0.2 U/mL of HRP, then incubate the samples in dark place at 37 °C for 1h using Krebs Ringer's phosphate glucose buffer (KRPG). After incubation, separate the buffer from the tissue, and measure fluorescence at 530 nm excitation (with an appropriate emission filter around 590 nm) [152,157]. This assay is highly sensitive, allowing for quantitative measurement of low concentrations of extracellular H_2O_2. However, it is important to protect the reaction from light and to optimize HRP concentration to avoid non-specific background signals.

17. Genetic Sensors for Mitochondrial ROS Measurement

Genetically encoded fluorescent biosensors have become precise and efficient tools to assess redox signaling and ROS dynamics within live cells. These protein-based sensors can be specifically targeted to cellular subcompartments, such as mitochondria, making them invaluable for studying localized ROS production, particularly mitochondrial H_2O_2 release [158,159]. Recent advances in biosensor technology have led to design of engineered probes that specifically and reliably detect H_2O_2. These probes offer key advantages such as high sensitivity, specificity reversibility and ability to enable real-time detection and visualization of redox flux under variety of physiological and pathological conditions. Two of the most widely used genetically encoded H_2O_2 sensors are roGFP2-Orp1 and HyPer [160–162]. roGFP2-Orp1is a redox-sensitive green fluorescent protein (roGFP) fused with the Orp1 peroxidase domain, enabling selective H_2O_2 detection through reversible oxidation. Whereas HyPer is a sensor derived from a permuted yellow fluorescent protein (cpYFP) fused to bacterial H_2O_2-sensing protein OxyR. It provides dynamic and ratiometric detection of intracellular H_2O_2 [163–165]. Both biosensors have been successfully studied in various cell types, including neurons, cardiomyocytes, and immune cells, allowing researchers to understand how ROS fluctuate in response to stimuli, drugs, or stress conditions. Their ability to monitor real-time oxidative events makes them a powerful complement to traditional chemical probes. [166–168].

18. In-Vivo Assays

18.1. Experimental In-Vivo Models

While in-silico and in-vitro models provide valuable insights into heart function in an isolated system outside the influence of physiological factors in a controlled experimental setting, it cannot replicate the complexity of a living organism. Therefore, in-vivo models remain essential for accurately studying the cardiovascular system and understanding key mechanisms of oxidative stress and DNA damage in a physiological context [169–172].

Effects of ROS induction in vivo can be directly modeled using a variety of chemical agents that either trigger free radicals' generation or disrupt mitochondrial and antioxidant defense systems. These compounds can lead to oxidative stress in a specific organ or in many cases systemic effects are observed leading to an animal model which can be utilized to study a specific scientific question.

18.2. Direct Inducers of Oxidative Stress In-Vivo

Oxidative stress can be experimentally triggered in an animal using chemical agents such as isoproterenol (ISO), a synthetic β-adrenergic agonist that mimics the effects of excessive sympathetic

 doi:10.20944/preprints202604.0024.v1

stimulation. Numerous studies have shown that ISO administration increases heart weight-to-body weight ratio, elevates serum levels of cardiac injury markers such as Aspartate Aminotransferase (AST), Creatine Kinase-MB Isoenzyme (CK-MB), Lactate Dehydrogenase (LDH), Malondialdehyde (MDA), Cardiac Troponin I (cTnI) and Creatine Phosphokinase (CPK) ,. It also leads to ST-segment elevation, reduced R-wave amplitude, QT interval prolongation and increased heart rate. In addition, it leads to structural damage like edema, and myocardial necrosis which can be observed via histology. This model is commonly used to study cardio-protective effects of antioxidant compounds ISO-induced myocardial infarction (MI) in both in-vitro and in-vivo settings [173,174]. To perform the study, the animals are divided into three major groups: a vehicle-control group, an ISO group receiving 85 mg/kg subcutaneously, and treatment groups receiving the test compound prior to ISO administration. The treatment group is used to evaluate the potential protective or therapeutic effects of the test compound against ISO-induced myocardial injury. ISO is typically administered for two consecutive days, and all animals are sacrificed or assessed 12 h after the final dose to analyze biochemical, histological, and functional parameters. One of the major drawbacks of such model is intense myocardial damage without involving vascular occlusion or chronic remodeling processes. Additionally, its outcomes can vary significantly with dose, strain, and systemic effects, limiting its translational relevance.

18.3. Doxorubicin (DOX)

Doxorubicin is an anthracycline chemotherapeutic agent known to induce dose-dependent cardiotoxicity. Its redox cycling within mitochondria results in the generation of superoxide and hydroxyl radicals, contributing to lipid peroxidation and mitochondrial damage. Repeated administration of DOX leads to progressive cardiac dysfunction, mimicking chronic heart failure.

In rodent models, DOX is administered intraperitoneally at cumulative doses of 10–20 mg/kg over 2–3 weeks. The protocol may involve a single high dose or multiple spaced doses to simulate chronic injury. Myocardium is particularly vulnerable to DOX as it targets mitochondrial function. Animals show reduced ejection fraction, increased oxidative markers, and fibrotic remodeling in cardiac tissue [175,176].

18.4. Carbon Tetrachloride (CCl_4)

CCl_4 is a potent hepatotoxin, but it also induces systemic oxidative stress, including in cardiac and renal tissues. It is metabolized by cytochrome P450 enzymes into trichloromethyl radicals that initiate lipid peroxidation.

In animal studies, CCl_4 is typically diluted 1:1 in olive oil and administered at 1–2 mL/kg intraperitoneally. The oxidative burden can be assessed in liver, heart, and serum through MDA levels, antioxidant enzyme activity, and histology [177,178]. Inflammatory mediators such as TNF-α, IL-1β, NF-κB activation leads to spillover from CCl_4 hepatotoxicity also damages myocardium in chronic condition.

18.5. Cisplatin

Cisplatin is a platinum-based chemotherapeutic agent widely used to induce nephrotoxicity in animal models. It impairs mitochondrial respiration, generates ROS, and depletes intracellular glutathione, particularly in renal tubular cells. It affects cardiac function but impacting cardio-renal cross-talk. Cisplatin is administered intraperitoneally at 5–10 mg/kg. Animals develop acute kidney injury, characterized by elevated serum creatinine, BUN, renal lipid peroxidation, and tubular necrosis [179,180].

18.6. Gentamicin

Gentamicin, an aminoglycoside antibiotic, causes oxidative damage primarily in the kidneys by accumulating in proximal tubules and generating mitochondrial superoxide.

 doi:10.20944/preprints202604.0024.v1

In rats, daily intraperitoneal administration of 80–120 mg/kg for 5–10 days induces nephrotoxicity, confirmed by raised creatinine, urea, and histological damage. Prolonged exposure to Gentamicin leads to oxidative stress in kidneys which increases lipid peroxidation and ROS. Histology of these animals would reveal cardiomyocyte vacuolization, edema and focal necrosis. Some reports demonstrated decreased heart rate and contractility. [181,182].

18.7. Bleomycin

Bleomycin is used to simulate oxidative lung injury and pulmonary fibrosis. Upon administration, it generates iron-catalyzed ROS that causes DNA strand breakage and release of inflammatory cytokine, which induces oxidative stress in cardiomyocytes indirectly.
The model involves a single intratracheal or intraperitoneal dose of 2–3 mg/kg. Within 7–14 days, animals exhibit impaired lung function, increased collagen deposition, and histological features of fibrosis [183,184].

18.8. Rotenone

Rotenone is a mitochondrial complex I inhibitor that impairs oxidative phosphorylation and increases intracellular ROS, especially in dopaminergic neurons. It is frequently used to model Parkinson's disease in vivo. Rotenone exposure upregulates oxidative-stress response genes in heart and elevates oxidative damage in heart mitochondria in rodent models, even when damage is subtle histologically. Animals receive chronic subcutaneous doses of 1–3 mg/kg for 4–6 weeks. Behavioral assessments reveal motor impairment, while brain tissue analysis confirms dopaminergic loss and oxidative damage [185,186].

18.9. Paraquat

Paraquat is a herbicide known for mitochondria-targeted redox cycler which interacts with complex I that generates ROS which leads to cute cardiac stress. Chronic exposure leads to metabolic programing and contractile defects in rodent models. Tempol pre-treatment partially reverses cardiac signatures making it a good mechanism to probe. In rodents, a single intraperitoneal dose of 10–20 mg/kg results in significant ROS generation, pulmonary edema, and myocardial necrosis upon long exposure [187,188].

18.10. Tert-Butyl Hydroperoxide (TBHP)

TBHP is a synthetic organic peroxide that undergoes heme-catalyzed decomposition leading to alkoxyl and peroxyl radical formation. These molecules directly cause lipid peroxidation and oxidative DNA damage. Cardiomyocytes are especially sensitive to TBHP due to high mitochondrial density and dependence on oxidative metabolism. TBHP is used to study acute oxidative stress, particularly in liver and kidney models. It is good model to study mechanistic redox studies but less translatable as compared to DOX or ISO models.
A single intraperitoneal dose of 2–5 mmol/kg leads to measurable oxidative injury within a few hours, often evident as increased MDA levels, reduced GSH, and histological damage [189,190].

18.11. Potassium Bromate ($KBrO_3$)

$KBrO_3$ is a strong oxidizing agent that generates reactive oxygen species and causes oxidative DNA damage, particularly in renal tissue. The signs of oxidative stress can be observed histologically in heart even though kidney is the classical target organ. In experimental models, oral or intraperitoneal administration of 100–200 mg/kg induces glomerular injury, proteinuria, and elevated lipid peroxidation markers [191].

18.12. Indirect Inducers of Oxidative Stress In-Vivo

 doi:10.20944/preprints202604.0024.v1

Oxidative stress can also develop indirectly in experimental animal models due to metabolic, inflammatory, psychological, or age-related imbalances that shift the redox system toward pro-oxidant dominance. These models do not rely on direct chemical pro-oxidants but instead trigger endogenous ROS production as a secondary effect of the biological process. They are increasingly used in translational research for diseases where oxidative stress is not the primary insult but a secondary consequence of systemic dysregulation [192].

18.13. High-Fat Diet (HFD)-Induced Metabolic Stress

Rodent model of high-fat diet (HFD) is commonly used to investigate oxidative stress resulting from metabolic syndrome. Chronic intake of saturated fats leads to insulin resistance, adipocyte hypertrophy, and mitochondrial dysfunction. This causes excessive ROS generation, mainly in liver, adipose tissue, and heart. Cardiac tissue due to high dependency on mitochondria is often impacted irreversibly. To generate the model, animals maintained on a 60% fat diet for 12–16 weeks exhibit increased levels of malondialdehyde (MDA), 4-hydroxynonenal (4-HNE), and reduced antioxidant enzyme activity in metabolic tissues. To evaluate therapeutic mechanisms, animals are split into two groups: a control group receiving normal chow and an HFD-fed group. Blood and tissues are collected at designated endpoints to assess oxidative damage and inflammation. Although the model recapitulates many features of human metabolic disease, inter-strain variability and the long duration required to establish significant pathology can be limitations [193,194].

18.14. Lipopolysaccharide (LPS)-Induced Systemic Inflammation

Lipopolysaccharide (LPS), a bacterial endotoxin, is widely used to initiate oxidative stress via systemic inflammation. LPS activates Toll-like receptor 4 (TLR4) on immune cells, leading to cytokine release, nitric oxide production, and ROS generation through NADPH oxidase. Elevated plasma levels of TNF-α, IL-6, nitric oxide, and protein carbonyls are commonly observed after LPS injection. To generate the model, animals are divided into a control group and an LPS group receiving a single intraperitoneal dose of 5 mg/kg. Tissues such as liver, lung, and brain are collected 6–24 hours post-administration for biochemical and histological evaluation. The LPS model is ideal for screening anti-inflammatory and antioxidant compounds under acute immune challenge. However, the short-lived nature of the response limits its relevance for chronic disease modeling [195].

18.15. D-Galactose-Induced Aging Model

D-galactose, when administered over extended periods, accelerates aging by promoting oxidative stress via the formation of advanced glycation end-products and mitochondrial dysfunction. Rats or mice receiving 100–150 mg/kg/day subcutaneously for 6–8 weeks show increased lipid peroxidation, protein oxidation, and decreased superoxide dismutase (SOD) activity in the brain, liver, and kidneys. The model is generated by assigning animals to control and D-galactose-treated groups. Behavioral assessments are often performed in parallel to examine cognitive effects, followed by tissue collection for oxidative biomarkers. This model is widely used in anti-aging and neurodegenerative studies. One drawback is that it mimics accelerated aging rather than natural senescence, which may not fully reflect chronic aging mechanisms

18.16. Hypoxia/Reoxygenation (H/R) Injury Model

Hypoxia followed by reoxygenation replicates ischemia-reperfusion injury, where a burst of ROS is generated upon oxygen restoration. This is primarily driven by mitochondrial electron transport chain instability, xanthine oxidase activation, and neutrophil infiltration. In myocardial or cerebral H/R models, oxidative stress is accompanied by elevated MDA, reduced GSH, and mitochondrial swelling. Cytokine response that follows the initial hypoxic insult often shapes the extent and prognosis of the injury [196]. To induce this model, rodents are subjected to controlled hypoxia (e.g., via coronary artery ligation or hypoxia chambers) for 30–60 minutes, followed by

 doi:10.20944/preprints202604.0024.v1

normoxic reoxygenation for 2–24 hours. Sham-operated animals serve as controls. This model effectively mirrors clinical scenarios such as myocardial infarction or stroke but requires surgical expertise and standardization [61,197].

18.17. Chronic Restraint Stress Model

Prolonged psychological stress is a recognized inducer of oxidative stress in the brain and cardiovascular system. It activates the hypothalamic–pituitary–adrenal axis, elevating glucocorticoid levels and altering redox signaling. Chronic restraint stress increases brain ROS levels, disrupts mitochondrial membrane potential, and decreases SOD and catalase activity in regions like the hippocampus. To induce the model, rodents are placed in plastic restrainers for 4–6 hours per day over 14–21 days. A control group is handled similarly without restraint. After the exposure period, behavioral assessments are followed by tissue analysis for oxidative markers. While highly relevant to stress-related disorders, variability in animal temperament and environmental sensitivity can affect reproducibility [198].

18.18. Sleep Deprivation Model

Sleep deprivation is associated with increased oxidative stress, especially in the central nervous system. Disrupted sleep leads to enhanced ROS production, impaired antioxidant defenses, and neuronal damage, particularly in memory-related regions like the hippocampus.

This model is implemented using gentle handling or rotating platform systems to prevent REM or total sleep for 24–72 hours. Following deprivation, animals show elevated brain MDA, decreased GSH, and impaired performance in behavioral tests. Control animals are housed under similar lighting and temperature conditions without intervention. Despite being non-invasive, the model demands continuous monitoring and often shows variability in stress levels induced by the setup itself [199].

18.19. Senescence-Accelerated Mouse Model (SAMP8)

The senescence-accelerated mouse prone 8 (SAMP8) strain is a spontaneous aging model that naturally exhibits increased oxidative stress, cognitive decline, and mitochondrial dysfunction at an early age. These mice show elevated brain MDA levels, increased protein oxidation, and reduced antioxidant enzyme expression by 5–6 months of age.

Unlike other models, no intervention is needed. Age-matched SAMR1 mice are used as controls. Tissues from brain, heart, and skeletal muscle are typically collected for biochemical and histological analysis. SAMP8 is well-established in aging research and provides a stable platform for long-term studies. However, genetic drift and cost of colony maintenance can be limiting factors [200,201].

19. In-Vivo Assays for Oxidative Stress and DNA Damage in Cardiovascular Diseases

19.1. Electrocardiography (ECG)

To perform ECG recordings, SD rats are anesthetized, and positioned supine approximately for 30 minutes. Next, acupuncture needle electrodes are inserted subcutaneously based on lead II configuration i.e., right foreleg, left foreleg and left rear leg. ECG signal and heart rate are recorded at every 1 min interval every 5 min using a PowerLab system, and data are analyzed by LabChart 7 software [174], special attention should be given to changes in the ST-segment, which can indicate ischemia or myocardial injury.

19.2. Biochemical Estimations

After blood collection, centrifuge and separate the serum. Next, following biomarkers should be measured by using commercially available kit. These are routinely used in laboratory settings.

 doi:10.20944/preprints202604.0024.v1

Troponin I (cTnI), Aspartate aminotransferase (AST), Creatine phosphokinase (CPK), Creatine kinase-MB isoenzyme (CK-MB), Lactate dehydrogenase (LDH), Malondialdehyde (MDA) should be measures as they can be indicative of myocardial injury and oxidative damage [202–205].

19.3. Histopathological Examination

For histopathological assessment, after rats are sacrificed in accordance with ethical guidelines and their hearts are excised, immediately fix them in 10% buffered formalin. The ventricular mass is sectioned longitudinally from the apex to the base, followed by routine dehydration with graded alcohol and clearing with xylene before embedding in paraffin wax. Thin histological sections of approximately 5 µm are then prepared by slicing the paraffin block using microtome. These sections are then stained with hematoxylin and eosin (H &E) and examined under the light microscope to evaluate changes in tissue architecture. Key structural and pathological changes such as Edema, cellular infiltration, and myocardial necrosis should be evaluated to understand the extent of myocardial damage [206–208]. Special stains can be performed on the consecutive paraffin sections to characterize the cellular subtypes in case of massive infiltration and restructuring. This examination plays a crucial role in assessing oxidative stress-induced myocardial damage, as oxidative injury often manifests histologically through features such as interstitial edema, inflammatory cell infiltration, and myocardial fiber necrosis. These structural changes are consistent with the downstream effects of reactive oxygen species (ROS) on cardiac tissue integrity and are commonly observed in oxidative stress-related models of myocardial injury.

20. Conclusion and Future Perspective

Oxidative stress plays a central role in the development and progression of many diseases yet studying it in a lab setting is not straightforward. Over the years, health care professionals have developed a wide variety of in-vitro and in-vivo models to replicate oxidative conditions, each with its own strengths and weaknesses. Direct chemical inducers like TBHP, ISO, or H_2O_2 offer quick and controlled induction of oxidative stress but often lack the complexity seen in actual disease states which is influenced by multiple factors. On the other hand, indirect models—like high-fat diets, LPS exposure, or aging-based setups—better reflect physiological conditions but the results can often vary depending on the dosage, exposure and strain background. What's often missing from the literature is a clear, side-by-side comparison of these models in one place. This review aims to fill that gap by compiling a detailed yet accessible overview of the most widely used oxidative stress models. It includes not only how these models are set up, but also what to expect in terms of biomarkers, tissue responses, and practical challenges. The addition of redox proteomics insights and models like the SAMP8 mouse helps connect molecular mechanisms to disease progression. By bringing together both direct and indirect inducers, this paper offers a practical toolkit for scientists designing studies in cardiovascular, metabolic, or neurodegenerative contexts. It encourages more thoughtful model selection based on research questions rather than convenience alone. In doing so, it bridges the gap between simplified systems and complex diseases. Ultimately, this review is meant to serve as a reference point—one that helps researchers navigate the crowded and sometimes confusing space of oxidative stress modeling.

Author Contributions Statement: S.G.: Conceptualization, writing of original draft preparation. P.P., H.Z.: Conceptualization, supervision, writing of original draft, reviewing & editing .E. M. O.: Supervision, writing, reviewing & editing.

Competing Interests: The authors declare that they have no known competing financial interests or personal relationships that could have appeared to influence the work reported in this paper.

References

 doi:10.20944/preprints202604.0024.v1

1. Flora, G.D. and M.K. Nayak, *A Brief Review of Cardiovascular Diseases, Associated Risk Factors and Current Treatment Regimes.* Curr Pharm Des, 2019. **25**(38): p. 4063–4084.
2. Dunbar, S.B., et al., *Projected Costs of Informal Caregiving for Cardiovascular Disease: 2015 to 2035: A Policy Statement From the American Heart Association.* Circulation, 2018. **137**(19): p. e558–e577.
3. Ruan, Y., et al., *Cardiovascular disease (CVD) and associated risk factors among older adults in six low-and middle-income countries: results from SAGE Wave 1.* BMC Public Health, 2018. **18**(1): p. 778.
4. Tsermpini, E.E., A. Plemenitaš Ilješ, and V. Dolžan, *Alcohol-Induced Oxidative Stress and the Role of Antioxidants in Alcohol Use Disorder: A Systematic Review.* Antioxidants (Basel), 2022. **11**(7).
5. Sambiagio, N., et al., *Associations between urinary biomarkers of oxidative stress and biomarkers of tobacco smoke exposure in smokers.* Sci Total Environ, 2022. **852**: p. 158361.
6. Pizzino, G., et al., *Oxidative Stress: Harms and Benefits for Human Health.* Oxid Med Cell Longev, 2017. **2017**: p. 8416763.
7. Dubois-Deruy, E., et al., *Oxidative Stress in Cardiovascular Diseases.* Antioxidants (Basel), 2020. **9**(9).
8. Othman, E.M., H. Hintzsche, and H. Stopper, *Signaling steps in the induction of genomic damage by insulin in colon and kidney cells.* Free Radic Biol Med, 2014. **68**: p. 247–57.
9. Snezhkina, A.V., et al., *ROS Generation and Antioxidant Defense Systems in Normal and Malignant Cells.* Oxid Med Cell Longev, 2019. **2019**: p. 6175804.
10. Othman, E.M., et al., *Metformin Protects Kidney Cells From Insulin-Mediated Genotoxicity* In Vitro *and in Male Zucker Diabetic Fatty Rats.* Endocrinology, 2016. **157**(2): p. 548–59.
11. D'Oria, R., et al., *The Role of Oxidative Stress in Cardiac Disease: From Physiological Response to Injury Factor.* Oxid Med Cell Longev, 2020. **2020**: p. 5732956.
12. Kurian, G.A., et al., *The Role of Oxidative Stress in Myocardial Ischemia and Reperfusion Injury and Remodeling: Revisited.* Oxid Med Cell Longev, 2016. **2016**: p. 1656450.
13. Antoniades, C., et al., *Oxidative stress, antioxidant vitamins, and atherosclerosis. From basic research to clinical practice.* Herz, 2003. **28**(7): p. 628–38.
14. Jové, M., et al., *The Advanced Lipoxidation End-Product Malondialdehyde-Lysine in Aging and Longevity.* Antioxidants (Basel), 2020. **9**(11).
15. Sanderson, K.J., et al., *Lipid peroxidation of circulating low density lipoproteins with age, smoking and in peripheral vascular disease.* Atherosclerosis, 1995. **118**(1): p. 45–51.
16. Nacítarhan, S., T. Özben, and N.e. Tuncer, *Serum and urine malondialdehyde levels in NIDDM patients with and without hyperlipidemia.* Free Radical Biology and Medicine, 1995. **19**(6): p. 893–896.
17. Garbern, J.C., C.L. Mummery, and R.T. Lee, *Model systems for cardiovascular regenerative biology.* Cold Spring Harb Perspect Med, 2013. **3**(4): p. a014019.
18. Capes-Davis, A., et al., *Cell Lines as Biological Models: Practical Steps for More Reliable Research.* Chem Res Toxicol, 2019. **32**(9): p. 1733–1736.
19. Field, L.J., *Atrial natriuretic factor-SV40 T antigen transgenes produce tumors and cardiac arrhythmias in mice.* Science, 1988. **239**(4843): p. 1029–33.
20. Claycomb, W.C., et al., *HL-1 cells: a cardiac muscle cell line that contracts and retains phenotypic characteristics of the adult cardiomyocyte.* Proc Natl Acad Sci U S A, 1998. **95**(6): p. 2979–84.
21. Davidson, M.M., et al., *Novel cell lines derived from adult human ventricular cardiomyocytes.* J Mol Cell Cardiol, 2005. **39**(1): p. 133–47.
22. Watkins, S.J., G.M. Borthwick, and H.M. Arthur, *The H9C2 cell line and primary neonatal cardiomyocyte cells show similar hypertrophic responses* in vitro. In Vitro Cell Dev Biol Anim, 2011. **47**(2): p. 125–31.
23. Ellingsen, O., et al., *Adult rat ventricular myocytes cultured in defined medium: phenotype and electromechanical function.* Am J Physiol, 1993. **265**(2 Pt 2): p. H747–54.
24. Mitcheson, J.S., J.C. Hancox, and A.J. Levi, *Cultured adult cardiac myocytes: future applications, culture methods, morphological and electrophysiological properties.* Cardiovasc Res, 1998. **39**(2): p. 280–300.
25. Moretti, A., et al., *Pluripotent stem cell models of human heart disease.* Cold Spring Harb Perspect Med, 2013. **3**(11).
26. Witek, P., et al., *The effect of a number of H9C2 rat cardiomyocytes passage on repeatability of cytotoxicity study results.* Cytotechnology, 2016. **68**(6): p. 2407–2415.

 doi:10.20944/preprints202604.0024.v1

27. Zordoky, B.N. and A.O. El-Kadi, *H9c2 cell line is a valuable* in vitro *model to study the drug metabolizing enzymes in the heart.* J Pharmacol Toxicol Methods, 2007. **56**(3): p. 317–22.
28. Kimes, B.W. and B.L. Brandt, *Properties of a clonal muscle cell line from rat heart.* Exp Cell Res, 1976. **98**(2): p. 367–81.
29. Curtis, M.W. and B. Russell, *Micromechanical regulation in cardiac myocytes and fibroblasts: implications for tissue remodeling.* Pflugers Arch, 2011. **462**(1): p. 105–17.
30. Cerbai, E., et al., *Isolated cardiac cells for electropharmacological studies.* Pharmacol Res, 2000. **42**(1): p. 1–8.
31. Ribeiro, A.J., et al., *Contractility of single cardiomyocytes differentiated from pluripotent stem cells depends on physiological shape and substrate stiffness.* Proc Natl Acad Sci U S A, 2015. **112**(41): p. 12705–10.
32. von Gise, A., et al., *YAP1, the nuclear target of Hippo signaling, stimulates heart growth through cardiomyocyte proliferation but not hypertrophy.* Proc Natl Acad Sci U S A, 2012. **109**(7): p. 2394–9.
33. Guo, L., et al., *Estimating the risk of drug-induced proarrhythmia using human induced pluripotent stem cell-derived cardiomyocytes.* Toxicol Sci, 2011. **123**(1): p. 281–9.
34. Lu, J., et al., *Improving cardiac conduction with a skeletal muscle sodium channel by gene and cell therapy.* J Cardiovasc Pharmacol, 2012. **60**(1): p. 88–99.
35. Chaicharoenaudomrung, N., P. Kunhorm, and P. Noisa, *Three-dimensional cell culture systems as an* in vitro *platform for cancer and stem cell modeling.* World J Stem Cells, 2019. **11**(12): p. 1065–1083.
36. Pontes Soares, C., et al., *2D and 3D-organized cardiac cells shows differences in cellular morphology, adhesion junctions, presence of myofibrils and protein expression.* PLoS One, 2012. **7**(5): p. e38147.
37. Shimizu, T., et al., *Fabrication of pulsatile cardiac tissue grafts using a novel 3-dimensional cell sheet manipulation technique and temperature-responsive cell culture surfaces.* Circ Res, 2002. **90**(3): p. e40.
38. Kirkpatrick, C.J., S. Fuchs, and R.E. Unger, *Co-culture systems for vascularization--learning from nature.* Adv Drug Deliv Rev, 2011. **63**(4-5): p. 291–9.
39. Mehling, M. and S. Tay, *Microfluidic cell culture.* Current Opinion in Biotechnology, 2014. **25**: p. 95–102.
40. Duell, B.L., et al., *Epithelial cell coculture models for studying infectious diseases: benefits and limitations.* J Biomed Biotechnol, 2011. **2011**: p. 852419.
41. Halldorsson, S., et al., *Advantages and challenges of microfluidic cell culture in polydimethylsiloxane devices.* Biosensors and Bioelectronics, 2015. **63**: p. 218–231.
42. Bi, Y.M., et al., *3,5-Dicaffeoylquinic acid protects H9C2 cells against oxidative stress-induced apoptosis via activation of the PI3K/Akt signaling pathway.* Food Nutr Res, 2018. **62**.
43. Fan, H.J., et al., *The role of ginsenoside Rb1, a potential natural glutathione reductase agonist, in preventing oxidative stress-induced apoptosis of H9C2 cells.* J Ginseng Res, 2020. **44**(2): p. 258–266.
44. Wu, Y.T., et al., *Tanshinone I Inhibits Oxidative Stress-Induced Cardiomyocyte Injury by Modulating Nrf2 Signaling.* Front Pharmacol, 2021. **12**: p. 644116.
45. T, M.M., T. Anand, and F. Khanum, *Attenuation of cytotoxicity induced by tBHP in H9C2 cells by Bacopa monniera and Bacoside A.* Pathophysiology, 2018. **25**(2): p. 143–149.
46. Han, S., et al., *Lotus Bee Pollen Extract Inhibits Isoproterenol-Induced Hypertrophy via JAK2/STAT3 Signaling Pathway in Rat H9c2 Cells.* Antioxidants (Basel), 2022. **12**(1).
47. Han, D., et al., *Jujuboside A Protects H9C2 Cells from Isoproterenol-Induced Injury via Activating PI3K/Akt/mTOR Signaling Pathway.* Evidence-Based Complementary and Alternative Medicine, 2016. **2016**: p. 9593716.
48. Fan, C., et al., *Qi-Li-Qiang-Xin Alleviates Isoproterenol-Induced Myocardial Injury by Inhibiting Excessive Autophagy via Activating AKT/mTOR Pathway.* Front Pharmacol, 2019. **10**: p. 1329.
49. Fan, C.L., et al., *Fuziline alleviates isoproterenol-induced myocardial injury by inhibiting ROS-triggered endoplasmic reticulum stress via PERK/eIF2α/ATF4/Chop pathway.* J Cell Mol Med, 2020. **24**(2): p. 1332–1344.
50. Ransy, C., et al., *Use of H(2)O(2) to Cause Oxidative Stress, the Catalase Issue.* Int J Mol Sci, 2020. **21**(23).
51. Coyle, C.H. and K.N. Kader, *Mechanisms of H2O2-induced oxidative stress in endothelial cells exposed to physiologic shear stress.* Asaio j, 2007. **53**(1): p. 17–22.
52. Anestopoulos, I., et al., *Silibinin protects H9c2 cardiac cells from oxidative stress and inhibits phenylephrine-induced hypertrophy: potential mechanisms.* J Nutr Biochem, 2013. **24**(3): p. 586–94.
53. Parsons, J.L. and J.K. Chipman, *The role of glutathione in DNA damage by potassium bromate* in vitro. Mutagenesis, 2000. **15**(4): p. 311–6.

 doi:10.20944/preprints202604.0024.v1

54. Watanabe, S., S. Togashi, and T. Fukui, *Contribution of nitric oxide to potassium bromate-induced elevation of methaemoglobin concentration in mouse blood.* Biol Pharm Bull, 2002. **25**(10): p. 1315–9.
55. Priscilla, D.H. and P.S. Prince, *Cardioprotective effect of gallic acid on cardiac troponin-T, cardiac marker enzymes, lipid peroxidation products and antioxidants in experimentally induced myocardial infarction in Wistar rats.* Chem Biol Interact, 2009. **179**(2-3): p. 118–24.
56. Oseni OA, Ogunmoyole T, and Idowu KA, *Lipid profile and cardio protective effects of aqueous extract of moringa oleifera (lam) leaf on bromate induced cardiotoxicity on Wistar albino rats.* European Journal of Advanced Research in Biological and Life Sciences, 2015. **3**: p. 52 66.
57. Kuo, S.C., et al., *Molecular mechanisms regarding potassium bromate-induced cardiac hypertrophy without apoptosis in H9c2 cells.* Mol Med Rep, 2018. **18**(5): p. 4700–4708.
58. Aggarwal, B.B., *Signalling pathways of the TNF superfamily: a double-edged sword.* Nat Rev Immunol, 2003. **3**(9): p. 745–56.
59. Yang, Y., et al., *Reactive oxygen species in the immune system.* Int Rev Immunol, 2013. **32**(3): p. 249–70.
60. Nishikawa, T., et al., *Normalizing mitochondrial superoxide production blocks three pathways of hyperglycaemic damage.* Nature, 2000. **404**(6779): p. 787–90.
61. Zorov, D.B., M. Juhaszova, and S.J. Sollott, *Mitochondrial ROS-induced ROS release: an update and review.* Biochim Biophys Acta, 2006. **1757**(5-6): p. 509–17.
62. Coppé, J.P., et al., *The senescence-associated secretory phenotype: the dark side of tumor suppression.* Annu Rev Pathol, 2010. **5**: p. 99–118.
63. Davies, M.J., *Detection of peroxyl and alkoxyl radicals produced by reaction of hydroperoxides with rat liver microsomal fractions.* Biochem J, 1989. **257**(2): p. 603–6.
64. Crane, D., et al., *Decreased flux through pyruvate dehydrogenase by thiol oxidation during t-butyl hydroperoxide metabolism in perfused rat liver.* Hoppe Seylers Z Physiol Chem, 1983. **364**(8): p. 977–87.
65. Park, J., et al., *NecroX-7 prevents oxidative stress-induced cardiomyopathy by inhibition of NADPH oxidase activity in rats.* Toxicol Appl Pharmacol, 2012. **263**(1): p. 1–6.
66. He, J., et al., *Oleuropein alleviates myocardial ischemia–reperfusion injury by suppressing oxidative stress and excessive autophagy via TLR4/MAPK signaling pathway.*
67. Song, L., et al., *Sulforaphane Attenuates Isoproterenol-Induced Myocardial Injury in Mice.* Biomed Res Int, 2020. **2020**: p. 3610285.
68. Zhang, H., et al., *Hirudin protects against isoproternol-induced myocardial infraction by alleviating oxidative via an Nrf2 dependent manner.* Int J Biol Macromol, 2020. **162**: p. 425–435.
69. Liu, F., et al., *STVNa Attenuates Isoproterenol-Induced Cardiac Hypertrophy Response through the HDAC4 and Prdx2/ROS/Trx1 Pathways.* Int J Mol Sci, 2020. **21**(2).
70. Sabeena Farvin, K.H., et al., *Effect of squalene on tissue defense system in isoproterenol-induced myocardial infarction in rats.* Pharmacol Res, 2004. **50**(3): p. 231–6.
71. Shao, Y., et al., *Novel rat model reveals important roles of β-adrenoreceptors in stress-induced cardiomyopathy.* Int J Cardiol, 2013. **168**(3): p. 1943–50.
72. Gavanji, S., et al., *Cytotoxic Activity of Herbal Medicines as Assessed* in Vitro*: A review.* Chem Biodivers, 2023.
73. Mu, R., et al., *Effects of Peroxiredoxin 6 and Its Mutants on the Isoproterenol Induced Myocardial Injury in H9C2 Cells and Rats.* Oxid Med Cell Longev, 2022. **2022**: p. 2576310.
74. Cinar, I., et al., In Vivo *and* In Vitro *Cardioprotective Effect of Gossypin Against Isoproterenol-Induced Myocardial Infarction Injury.* Cardiovasc Toxicol, 2022. **22**(1): p. 52–62.
75. Tan, M., et al., *Glutathione system enhancement for cardiac protection: pharmacological options against oxidative stress and ferroptosis.* Cell Death Dis, 2023. **14**(2): p. 131.
76. Piekarska, J., et al., *Effect of phytohaemagglutinin-P on apoptosis and necrosis in Trichinella spiralis infected mice.* Vet Parasitol, 2009. **159**(3-4): p. 240–4.
77. Jun, H.O., et al., *Clusterin protects H9c2 cardiomyocytes from oxidative stress-induced apoptosis via Akt/GSK-3β signaling pathway.* Exp Mol Med, 2011. **43**(1): p. 53–61.
78. Wan, C.R., et al., *Jujuboside A attenuates norepinephrine-induced apoptosis of H9c2 cardiomyocytes by modulating MAPK and AKT signaling pathways.* Mol Med Rep, 2018. **17**(1): p. 1132–1140.

 doi:10.20944/preprints202604.0024.v1

79. Chang, H., et al., *Luteolin Prevents H2O2-Induced Apoptosis in H9C2 Cells through Modulating Akt-P53/Mdm2 Signaling Pathway.* Biomed Res Int, 2016. **2016**: p. 5125836.
80. Li, H., et al., *Nuclear respiratory factor 1 protects H9C2 cells against hypoxia-induced apoptosis via the death receptor pathway and mitochondrial pathway.* Cell Biol Int, 2021. **45**(8): p. 1784–1796.
81. de Lima-Seolin, B.G., et al., *Bucindolol Modulates Cardiac Remodeling by Attenuating Oxidative Stress in H9c2 Cardiac Cells Exposed to Norepinephrine.* Oxid Med Cell Longev, 2019. **2019**: p. 6325424.
82. Li, M., et al., *Gas6 attenuates lipopolysaccharide-induced TNF-α expression and apoptosis in H9C2 cells through NF-κB and MAPK inhibition via the Axl/PI3K/Akt pathway.* Int J Mol Med, 2019. **44**(3): p. 982–994.
83. Li, F., et al., *Quercetin regulates inflammation, oxidative stress, apoptosis, and mitochondrial structure and function in H9C2 cells by promoting PVT1 expression.* Acta Histochem, 2021. **123**(8): p. 151819.
84. Luo, Q., et al., *3,3′-Diindolylmethane protects cardiomyocytes from LPS-induced inflammatory response and apoptosis.* BMC Pharmacol Toxicol, 2018. **19**(1): p. 71.
85. Zhang, Y., et al., *SENP3 protects H9C2 cells from apoptosis triggered by H/R via STAT3 pathway.* Eur Rev Med Pharmacol Sci, 2018. **22**(9): p. 2778–2786.
86. Huang, G., et al., *Secoisolariciresinol diglucoside prevents the oxidative stress-induced apoptosis of myocardial cells through activation of the JAK2/STAT3 signaling pathway.* Int J Mol Med, 2018. **41**(6): p. 3570–3576.
87. Han, X., et al., *Protective mechanisms of 10-gingerol against myocardial ischemia may involve activation of JAK2/STAT3 pathway and regulation of Ca(2+) homeostasis.* Biomed Pharmacother, 2022. **151**: p. 113082.
88. Zhao, L., L. Cheng, and Y. Wu, *Ambra1 Alleviates Hypoxia/Reoxygenation Injury in H9C2 Cells by Regulating Autophagy and Reactive Oxygen Species.* Biomed Res Int, 2020. **2020**: p. 3062689.
89. Zhang, Q., et al., *Plumbagin protects H9c2 cardiomyocytes against TBHP-induced cytotoxicity by alleviating ROS-induced apoptosis and modulating autophagy.* Exp Ther Med, 2022. **24**(2): p. 501.
90. Ma, L.Q., et al., *Sweroside Alleviated Aconitine-Induced Cardiac Toxicity in H9c2 Cardiomyoblast Cell Line.* Front Pharmacol, 2018. **9**: p. 1138.
91. Zheng, B., et al., *Mechanisms of cinnamic aldehyde against myocardial ischemia/hypoxia injury* in vivo *and* in vitro*: Involvement of regulating PI3K/AKT signaling pathway.* Biomed Pharmacother, 2022. **147**: p. 112674.
92. Mao, S., et al., *Role of PI3K/AKT/mTOR Pathway Associated Oxidative Stress and Cardiac Dysfunction in Takotsubo Syndrome.* Curr Neurovasc Res, 2020. **17**(1): p. 35–43.
93. Othman, E.M., et al., *The Plant Hormone Cytokinin Confers Protection against Oxidative Stress in Mammalian Cells.* PLoS One, 2016. **11**(12): p. e0168386.
94. Divakaruni, A.S., et al., *Chapter Sixteen - Analysis and Interpretation of Microplate-Based Oxygen Consumption and pH Data*, in *Methods in Enzymology*, A.N. Murphy and D.C. Chan, Editors. 2014, Academic Press. p. 309–354.
95. Muralimanoharan, S., et al., *MIR-210 modulates mitochondrial respiration in placenta with preeclampsia.* Placenta, 2012. **33**(10): p. 816–23.
96. Wang, M., et al., *Araloside C protects H9c2 cardiomyoblasts against oxidative stress via the modulation of mitochondrial function.* Biomedicine & Pharmacotherapy, 2019. **117**: p. 109143.
97. Yu, J., et al., *Mitochondrial dynamics modulation as a critical contribution for Shenmai injection in attenuating hypoxia/reoxygenation injury.* Journal of Ethnopharmacology, 2019. **237**: p. 9–19.
98. Huynh, G.T., et al., *Review: Nanomaterials for Reactive Oxygen Species Detection and Monitoring in Biological Environments.* Frontiers in Chemistry, 2021. **9**.
99. Koren, K., S.M. Borisov, and I. Klimant, *Stable optical oxygen sensing materials based on click-coupling of fluorinated platinum(II) and palladium(II) porphyrins—A convenient way to eliminate dye migration and leaching.* Sensors and Actuators B: Chemical, 2012. **169**: p. 173–181.
100. Lee, Y.E., R. Smith, and R. Kopelman, *Nanoparticle PEBBLE sensors in live cells and* in vivo*.* Annu Rev Anal Chem (Palo Alto Calif), 2009. **2**: p. 57–76.
101. Lee, Y.-E.K. and R. Kopelman, *Optical nanoparticle sensors for quantitative intracellular imaging.* WIREs Nanomedicine and Nanobiotechnology, 2009. **1**(1): p. 98–110.
102. Barone, P.W., R.S. Parker, and M.S. Strano, In Vivo *Fluorescence Detection of Glucose Using a Single-Walled Carbon Nanotube Optical Sensor: Design, Fluorophore Properties, Advantages, and Disadvantages.* Analytical Chemistry, 2005. **77**(23): p. 7556–7562.

 doi:10.20944/preprints202604.0024.v1

103. Wang, X., F. Li, and Y. Guo, *Recent Trends in Nanomaterial-Based Biosensors for Point-of-Care Testing.* Frontiers in Chemistry, 2020. **8**.
104. Lee, C.H., et al., *Chemical Imaging* in Vivo*: Photoacoustic-Based 4-Dimensional Chemical Analysis.* Analytical Chemistry, 2019. **91**(4): p. 2561–2569.
105. Kim, C., et al., *Deeply penetrating* in vivo *photoacoustic imaging using a clinical ultrasound array system.* Biomed Opt Express, 2010. **1**(1): p. 278–284.
106. Hariri, A., et al., *Molecular imaging of oxidative stress using an LED-based photoacoustic imaging system.* Sci Rep, 2019. **9**(1): p. 11378.
107. Ahn, J., et al., In vivo *photoacoustic monitoring of vasoconstriction induced by acute hyperglycemia.* Photoacoustics, 2023. **30**: p. 100485.
108. Jung, E., et al., *Molecularly Engineered Theranostic Nanoparticles for Thrombosed Vessels: H2O2-Activatable Contrast-Enhanced Photoacoustic Imaging and Antithrombotic Therapy.* ACS Nano, 2018. **12**(1): p. 392–401.
109. Chen, R., et al., *Chemiluminescent nanomicelles for imaging hydrogen peroxide and self-therapy in photodynamic therapy.* J Biomed Biotechnol, 2011. **2011**: p. 679492.
110. Lim, C.-K., et al., *Chemiluminescence-Generating Nanoreactor Formulation for Near-Infrared Imaging of Hydrogen Peroxide and Glucose Level* in vivo. Advanced Functional Materials, 2010. **20**(16): p. 2644–2648.
111. Dasari, M., et al., *Chemiluminescent PEG-PCL micelles for imaging hydrogen peroxide.* Journal of Biomedical Materials Research Part A, 2009. **89A**(3): p. 561–566.
112. Lee, D., et al., *Detection of hydrogen peroxide with chemiluminescent micelles.* Int J Nanomedicine, 2008. **3**(4): p. 471–6.
113. Lee, D., et al., In vivo *imaging of hydrogen peroxide with chemiluminescent nanoparticles.* Nature Materials, 2007. **6**(10): p. 765–769.
114. Wen, F., et al., *Horseradish Peroxidase Functionalized Fluorescent Gold Nanoclusters for Hydrogen Peroxide Sensing.* Analytical Chemistry, 2011. **83**(4): p. 1193–1196.
115. Shiang, Y.-C., C.-C. Huang, and H.-T. Chang, *Gold nanodot-based luminescent sensor for the detection of hydrogen peroxide and glucose.* Chemical Communications, 2009(23): p. 3437–3439.
116. Li, D.-W., et al., *CdSe/ZnS quantum dot–Cytochrome c bioconjugates for selective intracellular O2˙− sensing.* Chemical Communications, 2011. **47**(30): p. 8539–8541.
117. Wang, S., M.-Y. Han, and D. Huang, *Nitric Oxide Switches on the Photoluminescence of Molecularly Engineered Quantum Dots.* Journal of the American Chemical Society, 2009. **131**(33): p. 11692–11694.
118. Casanova, D., et al., *Single europium-doped nanoparticles measure temporal pattern of reactive oxygen species production inside cells.* Nature Nanotechnology, 2009. **4**(9): p. 581–585.
119. Auchinvole, C.A.R., et al., *Monitoring Intracellular Redox Potential Changes Using SERS Nanosensors.* ACS Nano, 2012. **6**(1): p. 888–896.
120. Chaichi, A., A. Prasad, and M.R. Gartia, *Raman Spectroscopy and Microscopy Applications in Cardiovascular Diseases: From Molecules to Organs.* Biosensors (Basel), 2018. **8**(4).
121. Kim, J.-Y., et al., *Highly selective* in-vivo *imaging of tumor as an inflammation site by ROS detection using hydrocyanine-conjugated, functional nano-carriers.* Journal of Controlled Release, 2011. **156**(3): p. 398–405.
122. Kim, G., et al., *Nanoencapsulation Method for High Selectivity Sensing of Hydrogen Peroxide inside Live Cells.* Analytical Chemistry, 2010. **82**(6): p. 2165–2169.
123. King, M. and R. Kopelman, *Development of a hydroxyl radical ratiometric nanoprobe.* Sensors and Actuators B: Chemical, 2003. **90**(1): p. 76–81.
124. Cao, Y., et al., *Ratiometric Singlet Oxygen Nano-optodes and Their Use for Monitoring Photodynamic Therapy Nanoplatforms.* Photochemistry and Photobiology, 2005. **81**(6): p. 1489–1498.
125. Hammond, V.J., et al., *An optical sensor for reactive oxygen species: encapsulation of functionalised silica nanoparticles into silicate nanoprobes to reduce fluorophore leaching.* Analyst, 2007. **133**(1): p. 71–75.
126. Tian, J., et al., *A Highly Selective, Cell-Permeable Fluorescent Nanoprobe for Ratiometric Detection and Imaging of Peroxynitrite in Living Cells.* Chemistry – A European Journal, 2011. **17**(24): p. 6626–6634.
127. Kim, S.-H., et al., *Encapsulation of Enzymes within Polymer Spheres To Create Optical Nanosensors for Oxidative Stress.* Analytical Chemistry, 2005. **77**(21): p. 6828–6833.

 doi:10.20944/preprints202604.0024.v1

128. Lee, H., et al., *Fluorescent Gold Nanoprobe Sensitive to Intracellular Reactive Oxygen Species.* Advanced Functional Materials, 2009. **19**(12): p. 1884–1890.
129. Guo, C., et al., *Direct electrochemistry of hemoglobin on carbonized titania nanotubes and its application in a sensitive reagentless hydrogen peroxide biosensor.* Biosensors and Bioelectronics, 2008. **24**(4): p. 819–824.
130. Hrapovic, S., et al., *Electrochemical Biosensing Platforms Using Platinum Nanoparticles and Carbon Nanotubes.* Analytical Chemistry, 2004. **76**(4): p. 1083–1088.
131. Yu, X., et al., *Peroxidase activity of enzymes bound to the ends of single-wall carbon nanotube forest electrodes.* Electrochemistry Communications, 2003. **5**(5): p. 408–411.
132. Zeng, X., et al., *A third-generation hydrogen peroxide biosensor based on horseradish peroxidase immobilized on DNA functionalized carbon nanotubes.* Biosensors and Bioelectronics, 2009. **25**(4): p. 896–900.
133. Wang, J., *Carbon-Nanotube Based Electrochemical Biosensors: A Review.* Electroanalysis, 2005. **17**(1): p. 7–14.
134. Balasubramanian, K. and M. Burghard, *Biosensors based on carbon nanotubes.* Analytical and Bioanalytical Chemistry, 2006. **385**(3): p. 452–468.
135. Besteman, K., et al., *Enzyme-Coated Carbon Nanotubes as Single-Molecule Biosensors.* Nano Letters, 2003. **3**(6): p. 727–730.
136. Xu, J.-Z., et al., *An Amperometric Biosensor Based on the Coimmobilization of Horseradish Peroxidase and Methylene Blue on a Carbon Nanotubes Modified Electrode.* Electroanalysis, 2003. **15**(3): p. 219–224.
137. Vaneev, A.N., et al., In Vitro *and* In Vivo *Electrochemical Measurement of Reactive Oxygen Species After Treatment with Anticancer Drugs.* Analytical Chemistry, 2020. **92**(12): p. 8010–8014.
138. He, R., et al., *Electrochemical Visualization of Intracellular Hydrogen Peroxide at Single Cells.* Analytical Chemistry, 2016. **88**(4): p. 2006–2009.
139. Clausmeyer, J. and W. Schuhmann, *Nanoelectrodes: Applications in electrocatalysis, single-cell analysis and high-resolution electrochemical imaging.* TrAC Trends in Analytical Chemistry, 2016. **79**: p. 46–59.
140. Zhang, X.-W., et al., *Electrochemical Monitoring of ROS/RNS Homeostasis Within Individual Phagolysosomes Inside Single Macrophages.* Angewandte Chemie International Edition, 2019. **58**(23): p. 7753–7756.
141. Li, Y., et al., *Direct Electrochemical Measurements of Reactive Oxygen and Nitrogen Species in Nontransformed and Metastatic Human Breast Cells.* Journal of the American Chemical Society, 2017. **139**(37): p. 13055–13062.
142. Wang, Y., et al., *Nanoelectrodes for determination of reactive oxygen and nitrogen species inside murine macrophages.* Proceedings of the National Academy of Sciences, 2012. **109**(29): p. 11534–11539.
143. Jiang, H., et al., *Electrochemical Monitoring of Paclitaxel-Induced ROS Release from Mitochondria inside Single Cells.* Small, 2019. **15**(48): p. 1901787.
144. Actis, P., et al., *Electrochemical Nanoprobes for Single-Cell Analysis.* ACS Nano, 2014. **8**(1): p. 875–884.
145. Erofeev, A., et al., *Novel method for rapid toxicity screening of magnetic nanoparticles.* Scientific Reports, 2018. **8**(1): p. 7462.
146. Akasov, R.A., et al., *Photodynamic therapy of melanoma by blue-light photoactivation of flavin mononucleotide.* Scientific Reports, 2019. **9**(1): p. 9679.
147. Dikalov, S.I., et al., *Cellular accumulation and antioxidant activity of acetoxymethoxycarbonyl pyrrolidine nitroxides.* Free Radic Res, 2018. **52**(3): p. 339–350.
148. Dikalov, S.I. and D.G. Harrison, *Methods for detection of mitochondrial and cellular reactive oxygen species.* Antioxid Redox Signal, 2014. **20**(2): p. 372–82.
149. Hawkins, C.L. and M.J. Davies, *Detection and characterisation of radicals in biological materials using EPR methodology.* Biochimica et Biophysica Acta (BBA) - General Subjects, 2014. **1840**(2): p. 708–721.
150. Ouari, O., et al., *Recent developments and applications of the coupled EPR/Spin trapping technique (EPR/ST)*, in *Electron Paramagnetic Resonance: Volume 22*. 2011, The Royal Society of Chemistry. p. 1–40.
151. Dikalov, S.I., Y.F. Polienko, and I. Kirilyuk, *Electron Paramagnetic Resonance Measurements of Reactive Oxygen Species by Cyclic Hydroxylamine Spin Probes.* Antioxid Redox Signal, 2018. **28**(15): p. 1433–1443.
152. Dikalov, S., K.K. Griendling, and D.G. Harrison, *Measurement of Reactive Oxygen Species in Cardiovascular Studies.* Hypertension, 2007. **49**(4): p. 717–727.
153. Dikalov, S.I., et al., *EPR detection of cellular and mitochondrial superoxide using cyclic hydroxylamines.* Free Radic Res, 2011. **45**(4): p. 417–30.

 doi:10.20944/preprints202604.0024.v1

154. Kozuleva, M., et al., *Quantification of superoxide radical production in thylakoid membrane using cyclic hydroxylamines.* Free Radical Biology and Medicine, 2015. **89**: p. 1014–1023.
155. Israeli, A., et al., *Kinetics and mechanism of the comproportionation reaction between oxoammonium cation and hydroxylamine derived from cyclic nitroxides.* Free Radical Biology and Medicine, 2005. **38**(3): p. 317–324.
156. Zhou, M., et al., *A Stable Nonfluorescent Derivative of Resorufin for the Fluorometric Determination of Trace Hydrogen Peroxide: Applications in Detecting the Activity of Phagocyte NADPH Oxidase and Other Oxidases.* Analytical Biochemistry, 1997. **253**(2): p. 162–168.
157. Weber, D.S., et al., *Angiotensin II-induced hypertrophy is potentiated in mice overexpressing p22phox in vascular smooth muscle.* American Journal of Physiology-Heart and Circulatory Physiology, 2005. **288**(1): p. H37–H42.
158. Belousov, V.V., et al., *Genetically encoded fluorescent indicator for intracellular hydrogen peroxide.* Nature Methods, 2006. **3**(4): p. 281–286.
159. Gutscher, M., et al., *Proximity-based Protein Thiol Oxidation by H2O2-scavenging Peroxidases*.* Journal of Biological Chemistry, 2009. **284**(46): p. 31532–31540.
160. Ermakova, Y.G., et al., *Red fluorescent genetically encoded indicator for intracellular hydrogen peroxide.* Nature Communications, 2014. **5**(1): p. 5222.
161. Gibhardt, C.S., et al., *Imaging calcium and redox signals using genetically encoded fluorescent indicators.* Cell Calcium, 2016. **60**(2): p. 55–64.
162. Hernández-Barrera, A., et al., *Chapter Fifteen - Using Hyper as a Molecular Probe to Visualize Hydrogen Peroxide in Living Plant Cells: A Method with Virtually Unlimited Potential in Plant Biology*, in *Methods in Enzymology*, E. Cadenas and L. Packer, Editors. 2013, Academic Press. p. 275–290.
163. Zhuravlev, A., et al., *HyPer as a tool to determine the reductive activity in cellular compartments.* Redox Biol, 2024. **70**: p. 103058.
164. Hernández-Barrera, A., et al., *Using hyper as a molecular probe to visualize hydrogen peroxide in living plant cells: a method with virtually unlimited potential in plant biology.* Methods Enzymol, 2013. **527**: p. 275–90.
165. Nietzel, T., et al., *The fluorescent protein sensor roGFP2-Orp1 monitors* in vivo *H(2) O(2) and thiol redox integration and elucidates intracellular H(2) O(2) dynamics during elicitor-induced oxidative burst in Arabidopsis.* New Phytol, 2019. **221**(3): p. 1649–1664.
166. Arnaud, D., M.J. Deeks, and N. Smirnoff, *Organelle-targeted biosensors reveal distinct oxidative events during pattern-triggered immune responses.* Plant Physiol, 2023. **191**(4): p. 2551–2569.
167. Gutscher, M., et al., *Proximity-based protein thiol oxidation by H2O2-scavenging peroxidases.* J Biol Chem, 2009. **284**(46): p. 31532–40.
168. Rampon, C., et al., *Hydrogen Peroxide and Redox Regulation of Developments.* Antioxidants (Basel), 2018. **7**(11).
169. Neely, J.R., et al., *Effects of ischemia on function and metabolism of the isolated working rat heart.* Am J Physiol, 1973. **225**(3): p. 651–8.
170. Vidavalur, R., et al., Ex vivo *and* in vivo *approaches to study mechanisms of cardioprotection targeting ischemia/reperfusion (i/r) injury: useful techniques for cardiovascular drug discovery.* Curr Drug Discov Technol, 2008. **5**(4): p. 269–78.
171. Halapas, A., et al., In vivo *models for heart failure research.* In Vivo, 2008. **22**(6): p. 767–80.
172. Liang, J., et al., *Roles of Reactive Oxygen Species in Cardiac Differentiation, Reprogramming, and Regenerative Therapies.* Oxid Med Cell Longev, 2020. **2020**: p. 2102841.
173. Sajid, A., et al., *Cardioprotective Potential of Aqueous Extract of Fumaria indica on Isoproterenol-Induced Myocardial Infarction in SD Rats.* Oxid Med Cell Longev, 2022. **2022**: p. 2112956.
174. Tiwari, R., et al., *Cardioprotective potential of myricetin in isoproterenol-induced myocardial infarction in Wistar rats.* Phytother Res, 2009. **23**(10): p. 1361–6.
175. Octavia, Y., et al., *Doxorubicin-induced cardiomyopathy: from molecular mechanisms to therapeutic strategies.* J Mol Cell Cardiol, 2012. **52**(6): p. 1213–25.
176. Vejpongsa, P. and E.T. Yeh, *Prevention of anthracycline-induced cardiotoxicity: challenges and opportunities.* J Am Coll Cardiol, 2014. **64**(9): p. 938–45.
177. Weber, L.W., M. Boll, and A. Stampfl, *Hepatotoxicity and mechanism of action of haloalkanes: carbon tetrachloride as a toxicological model.* Crit Rev Toxicol, 2003. **33**(2): p. 105–36.

 doi:10.20944/preprints202604.0024.v1

178. Rechnagel, R.O. and E.A. Glende, Jr., *Carbon tetrachloride hepatotoxicity: an example of lethal cleavage.* CRC Crit Rev Toxicol, 1973. **2**(3): p. 263–97.
179. Chirino, Y.I. and J. Pedraza-Chaverri, *Role of oxidative and nitrosative stress in cisplatin-induced nephrotoxicity.* Exp Toxicol Pathol, 2009. **61**(3): p. 223–42.
180. Yao, X., et al., *Cisplatin nephrotoxicity: a review.* Am J Med Sci, 2007. **334**(2): p. 115–24.
181. Rodríguez-Barbero, A., et al., *Gentamicin nephrotoxicity in rats is not modified by verapamil.* Arch Int Physiol Biochim Biophys, 1993. **101**(6): p. 395–7.
182. Balakumar, P., A. Rohilla, and A. Thangathirupathi, *Gentamicin-induced nephrotoxicity: Do we have a promising therapeutic approach to blunt it?* Pharmacol Res, 2010. **62**(3): p. 179–86.
183. Moeller, A., et al., *The bleomycin animal model: a useful tool to investigate treatment options for idiopathic pulmonary fibrosis?* Int J Biochem Cell Biol, 2008. **40**(3): p. 362–82.
184. Chaudhary, N.I., A. Schnapp, and J.E. Park, *Pharmacologic differentiation of inflammation and fibrosis in the rat bleomycin model.* Am J Respir Crit Care Med, 2006. **173**(7): p. 769–76.
185. Cannon, J.R. and J.T. Greenamyre, *The role of environmental exposures in neurodegeneration and neurodegenerative diseases.* Toxicol Sci, 2011. **124**(2): p. 225–50.
186. Betarbet, R., et al., *Chronic systemic pesticide exposure reproduces features of Parkinson's disease.* Nat Neurosci, 2000. **3**(12): p. 1301–6.
187. Bus, J.S. and J.E. Gibson, *Paraquat: model for oxidant-initiated toxicity.* Environ Health Perspect, 1984. **55**: p. 37–46.
188. Dinis-Oliveira, R.J., et al., *Paraquat exposure as an etiological factor of Parkinson's disease.* Neurotoxicology, 2006. **27**(6): p. 1110–22.
189. Comporti, M., *Lipid peroxidation and cellular damage in toxic liver injury.* Lab Invest, 1985. **53**(6): p. 599–623.
190. Yagi, K., *Lipid peroxides and human diseases.* Chem Phys Lipids, 1987. **45**(2-4): p. 337–51.
191. Kurokawa, Y., et al., *Toxicity and carcinogenicity of potassium bromate--a new renal carcinogen.* Environ Health Perspect, 1990. **87**: p. 309–35.
192. Doridot, L., et al., *Implication of oxidative stress in the pathogenesis of systemic sclerosis via inflammation, autoimmunity and fibrosis.* Redox Biol, 2019. **25**: p. 101122.
193. Furukawa, S., et al., *Increased oxidative stress in obesity and its impact on metabolic syndrome.* J Clin Invest, 2004. **114**(12): p. 1752–61.
194. McGregor, R.A., et al., *Time-course microarrays reveal modulation of developmental, lipid metabolism and immune gene networks in intrascapular brown adipose tissue during the development of diet-induced obesity.* Int J Obes (Lond), 2013. **37**(12): p. 1524–31.
195. Park, B.S. and J.O. Lee, *Recognition of lipopolysaccharide pattern by TLR4 complexes.* Exp Mol Med, 2013. **45**(12): p. e66.
196. Heinen, A., et al., *IGF1 Treatment Improves Cardiac Remodeling after Infarction by Targeting Myeloid Cells.* Mol Ther, 2019. **27**(1): p. 46–58.
197. Kalogeris, T., et al., *Cell biology of ischemia/reperfusion injury.* Int Rev Cell Mol Biol, 2012. **298**: p. 229–317.
198. Madrigal, J.L., et al., *Glutathione depletion, lipid peroxidation and mitochondrial dysfunction are induced by chronic stress in rat brain.* Neuropsychopharmacology, 2001. **24**(4): p. 420–9.
199. Everson, C.A., C.D. Laatsch, and N. Hogg, *Antioxidant defense responses to sleep loss and sleep recovery.* Am J Physiol Regul Integr Comp Physiol, 2005. **288**(2): p. R374–83.
200. Butterfield, D.A. and D. Boyd-Kimball, *Redox proteomics and amyloid β-peptide: insights into Alzheimer disease.* J Neurochem, 2019. **151**(4): p. 459–487.
201. Takeda, T., *Senescence-accelerated mouse (SAM): a biogerontological resource in aging research.* Neurobiol Aging, 1999. **20**(2): p. 105–10.
202. Mihara, M. and M. Uchiyama, *Determination of malonaldehyde precursor in tissues by thiobarbituric acid test.* Anal Biochem, 1978. **86**(1): p. 271–8.
203. Karmen, A., F. Wroblewski, and J.S. Ladue, *Transaminase activity in human blood.* J Clin Invest, 1955. **34**(1): p. 126–31.

 doi:10.20944/preprints202604.0024.v1

204. Rajadurai, M. and P. Stanely Mainzen Prince, *Preventive effect of naringin on cardiac markers, electrocardiographic patterns and lysosomal hydrolases in normal and isoproterenol-induced myocardial infarction in Wistar rats.* Toxicology, 2007. **230**(2-3): p. 178–88.
205. Macdonald, R.P., J.R. Simpson, and E. Nossal, *Serum lactic dehydrogenase; a diagnostic aid in myocardial infarction.* J Am Med Assoc, 1957. **165**(1): p. 35–40.
206. Molh, A.K., et al., *Histopathological studies of cardiac lesions after an acute high dose administration of methamphetamine.* Malays J Med Sci, 2008. **15**(1): p. 23–30.
207. Liao, W., et al., *Cariporide Attenuates Doxorubicin-Induced Cardiotoxicity in Rats by Inhibiting Oxidative Stress, Inflammation and Apoptosis Partly Through Regulation of Akt/GSK-3β and Sirt1 Signaling Pathway.* Front Pharmacol, 2022. **13**: p. 850053.
208. Othmène, Y.B., et al., *Tebuconazole induced oxidative stress and histopathological alterations in adult rat heart.* Pestic Biochem Physiol, 2020. **170**: p. 104671.